SUPPORTING INFORMATION

Aggregation induced emission (AIE) active cross-linked poly(*N*-isopropyl acrylamide-co-tetra(phenyl)ethene di-acrylates): Sensors for effective nitroaromatics detection in aqueous environment

Feng Liu,[a] Yi Ren,[a] Hazel Lau,[a] Ben Zhong Tang*[b] and Hui Zhou*[a]

[a]Institute of Materials Research and Engineering, A*STAR (Agency for Science, Technology and Research), 2 Fusionopolis Way, Innovis, #08-03, Singapore 138634, Republic of Singapore.

[b]Department of Chemistry, The Hong Kong University of Science & Technology, Clear Water Bay, Kowloon, Hong Kong, China.

*Corresponding author: Hui Zhou and Ben Zhong Tang
Email address: chmzhouh@gmail.com; tangbenz@ust.hk

Mailing address: 2 Fusionopolis Way, Innovis, #08-03, Singapore 138634.

Tel: 65-6872-7543

Fax: 65-6872-7528

Table content

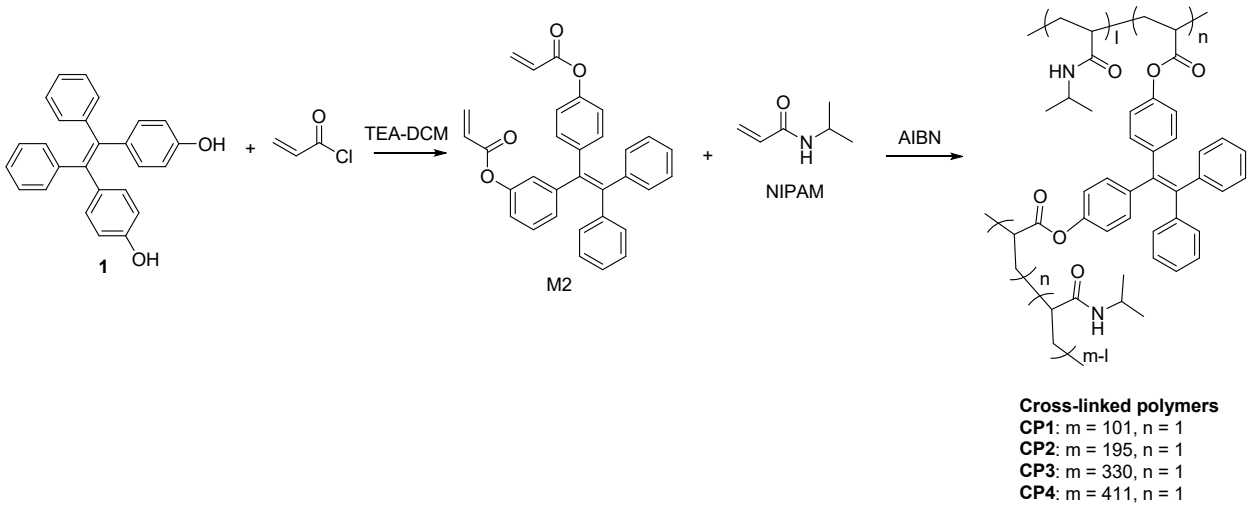

Scheme S1. Synthetic routes of monomers (**M2**)[1] and corresponding cross-linked polymers (**CP1-4**).

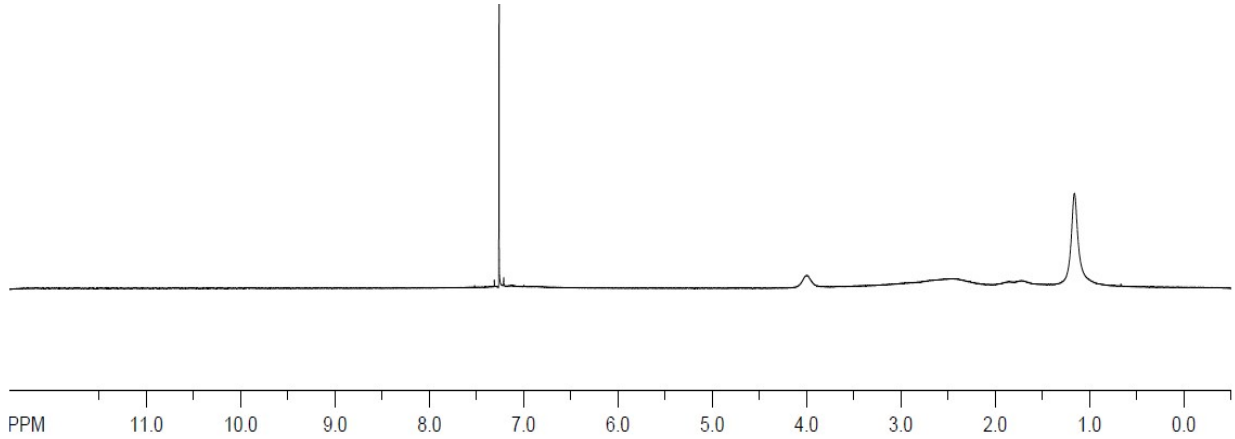

Figure S1. ^{1}H NMR spectrum of **CP1** in $CDCl_3$.

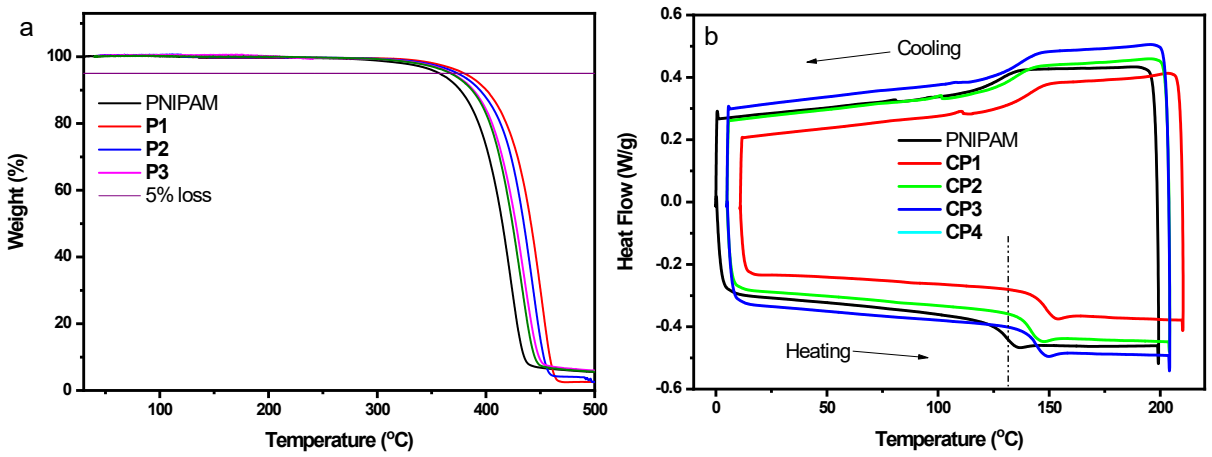

igure S2. (a) TGA thermograms of PNIPAM and **CP1-4** recorded under nitrogen at a heating rate of 20 °C/min. (b) DSC thermograms of PNIPAM and **CP1-4** recorded under nitrogen at a heating rate of 10 °C/min.

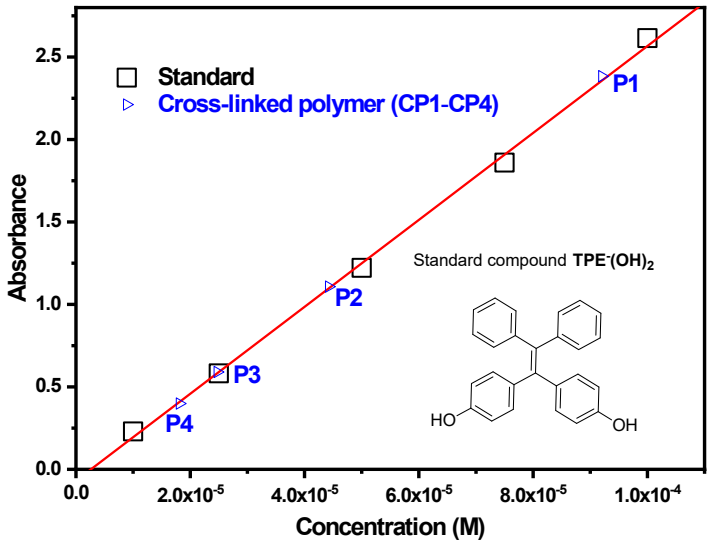

Figure S3. Calibration curve for determination of copolymer composition, using 4,4'-(2,2-diphenylethene-1,1-diyl)diphenol (TPE-$(OH)_2$) as standard. [TPE-$(OH)_2$] = 10^{-5} to 10^{-4} M, [PNIPAM] = 0.50 mg/mL, 20 °C. Open squares and circles are the data points for the standard and the copolymers, respectively.

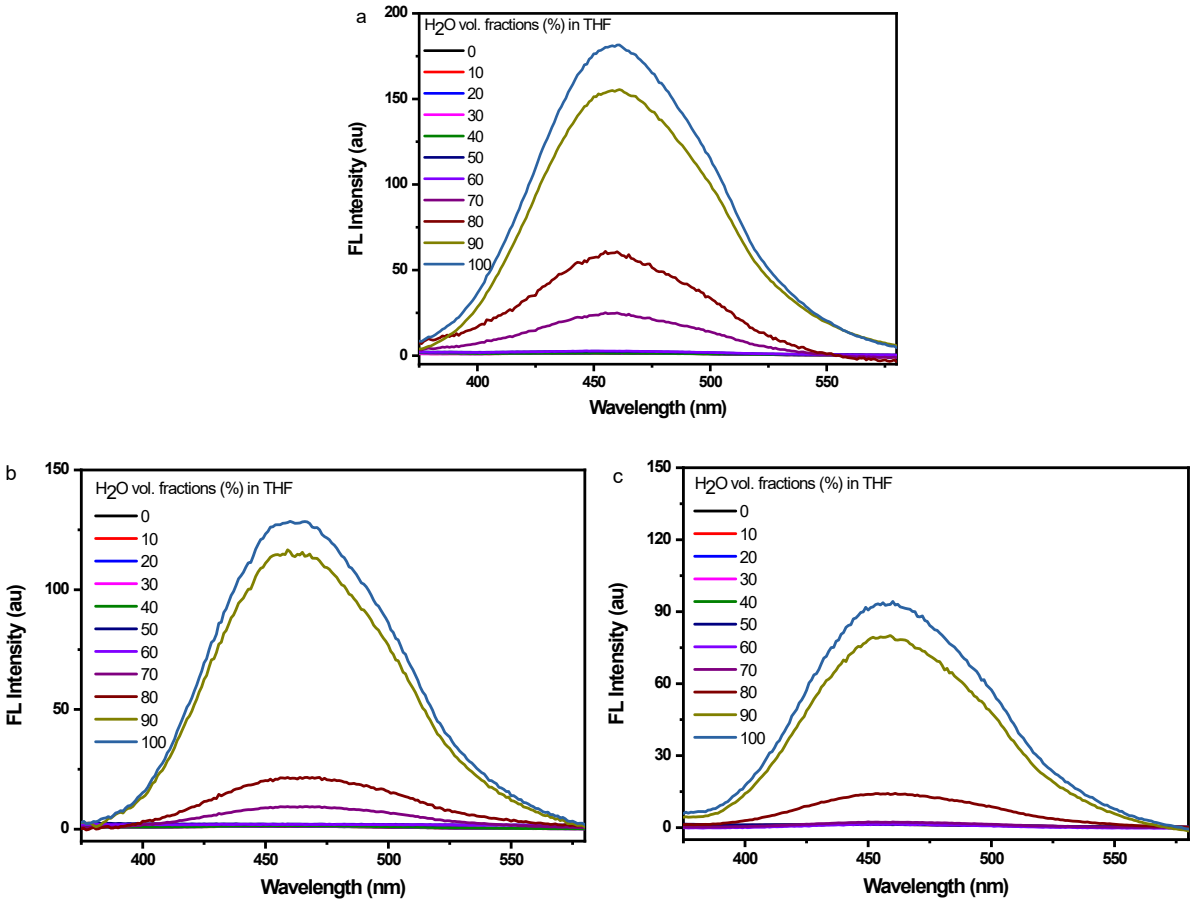

Figure S4. Fluorescence spectra of cross-linked polymers in THF/H_2O mixtures (λ_{ex} = 315 nm, [polymer] = 0.5 mg/mL, 20 °C): (a) **CP2**, (b) **CP3** and (c) **CP4**.

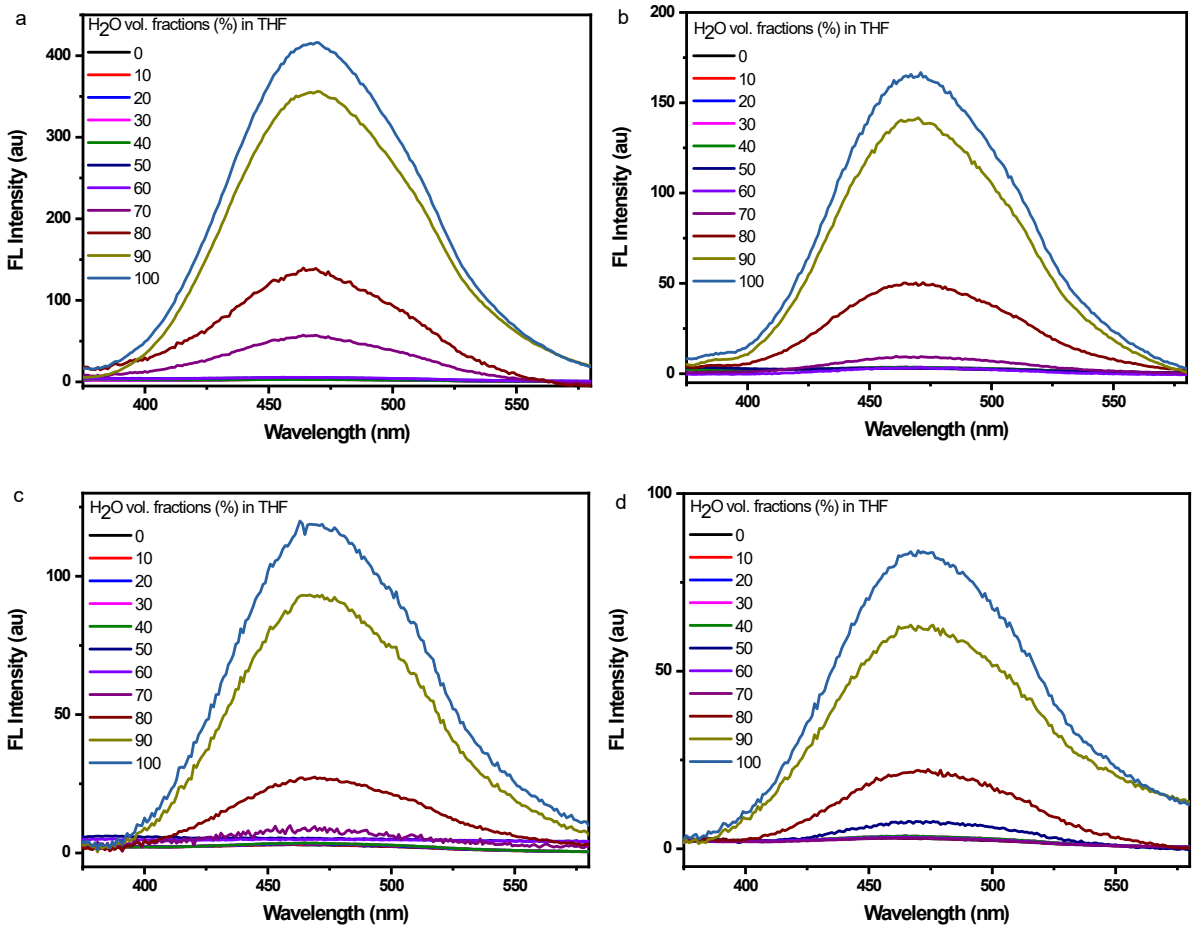

Figure S5. Fluorescence spectra of linear polymers in THF/H_2O mixtures (λ_{ex} = 318 nm, [polymer] = 0.5 mg/mL, 20 °C): (a) **LP1**, (b) **LP2**, c) **LP3** and (d) **LP4**.

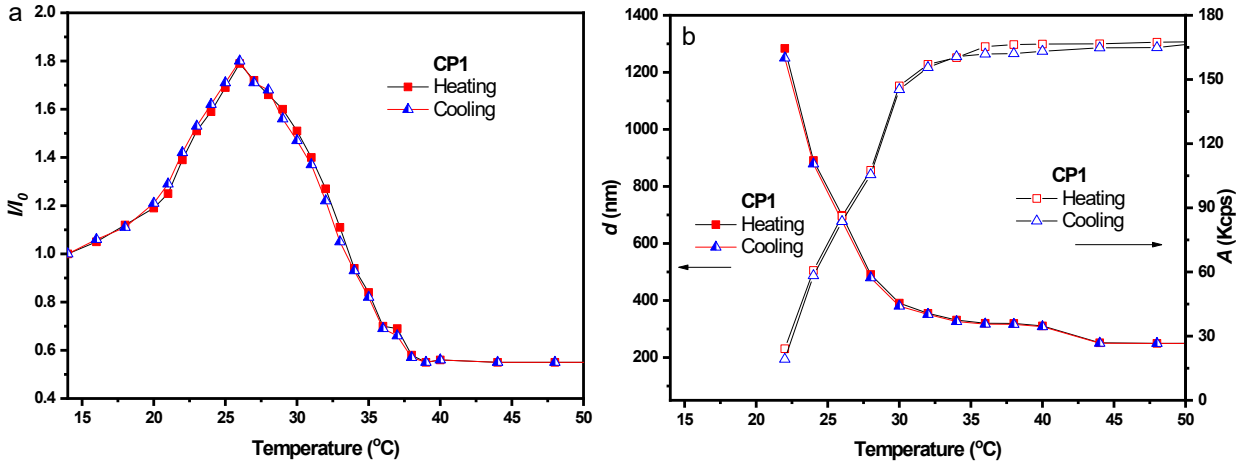

Figure S6. (a) Plot of I/I_0 *vs* temperature of **CP1**. (b) The particle size and solution turbidity (kcps) *vs* temperature of **CP1**. [**CP1**] = 0.5 mg/mL, I_0 and I are the fluorescence intensity at 14 °C and a measured temperature, respectively. The fluorescence intensity was recorded at 461 nm; λ_{ex} = 315 nm.

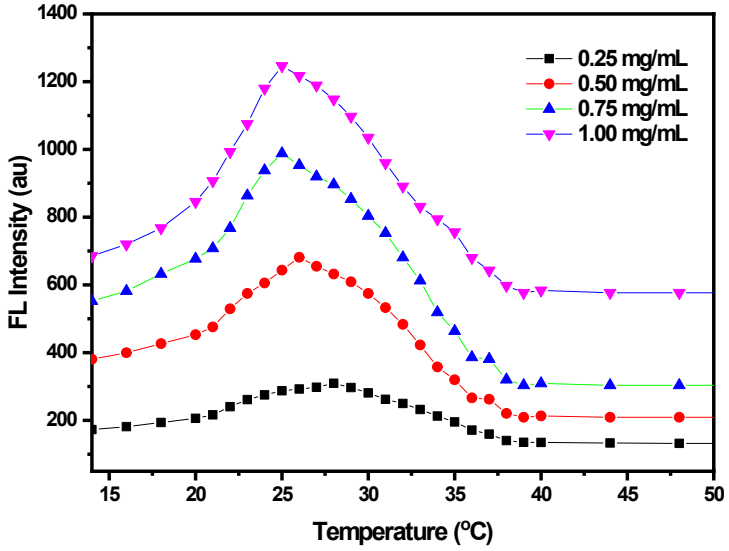

Figure S7. Plot of fluorescence intensity *vs* temperature of **CP1** with different concentration in H_2O. Concentration of copolymers **CP1** is 0.25, 0.50 and 1.0 mg/mL, respectively. Fluorescence was measured at 461 nm, excited at 315 nm.

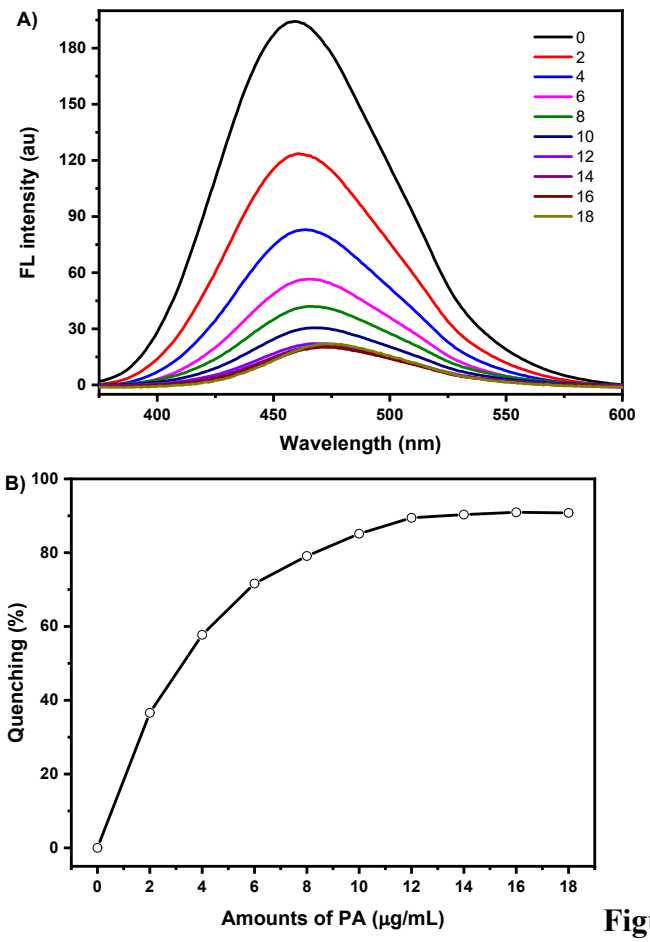

Figure S8. (A) Fluorescence spectra of 50.0 μg•mL^{-1} **CP1** in H_2O in the presence of different PA concentrations (μg•mL^{-1}). (B) Concentration-dependent fluorescence quenching of **CP1** by PA.

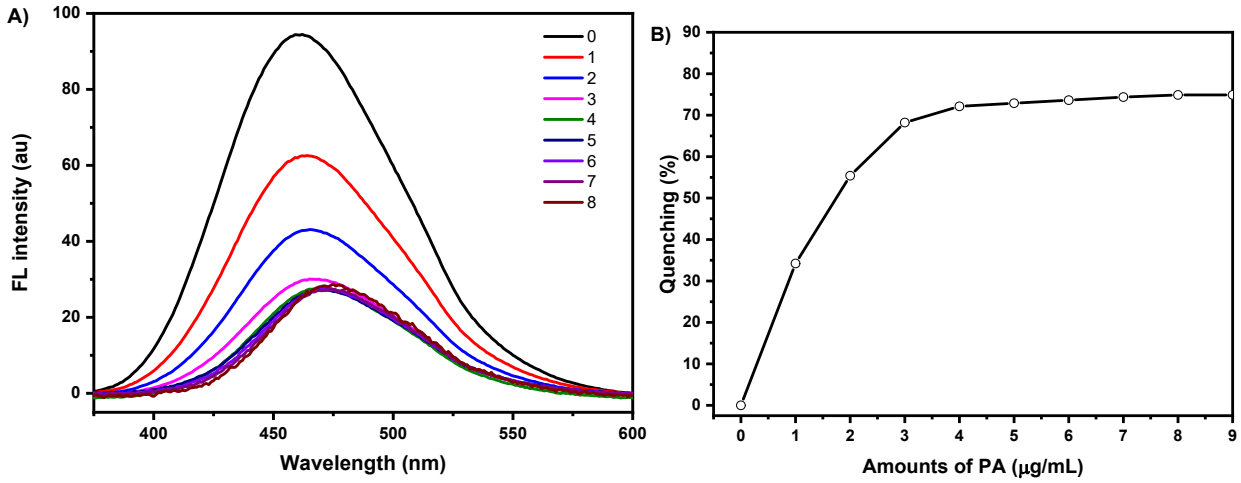

Figure S9. Fluorescence spectra of 25.0 μg•mL^{-1} **CP1** in H_2O in the presence of different PA concentrations (μg•mL^{-1}). (B) Concentration-dependent fluorescence quenching of **CP1** by PA.

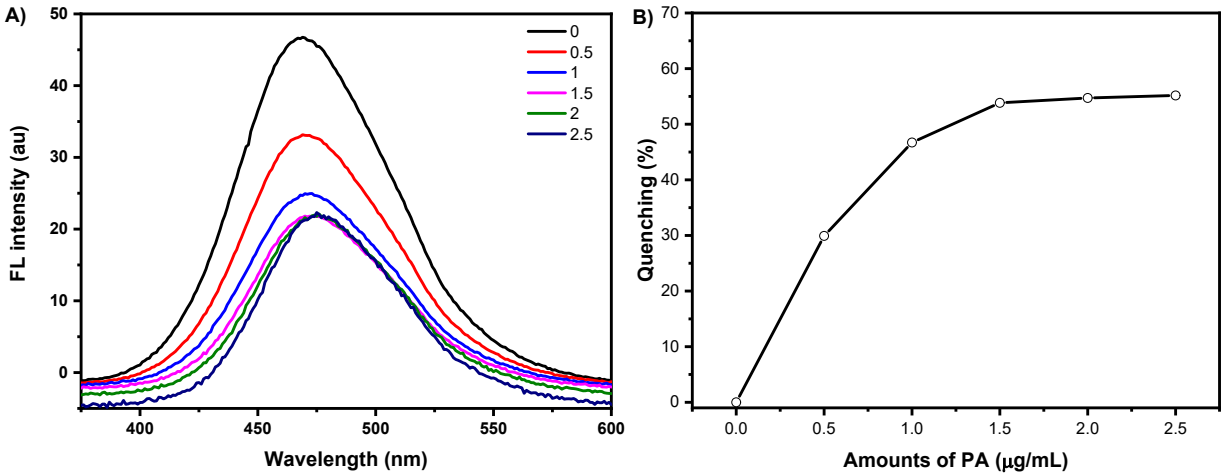

Figure S10. Fluorescence spectra of 12.5 μg•mL^{-1} **CP1** in H_2O in the presence of different PA concentrations (μg•mL^{-1}). (B) Concentration-dependent fluorescence quenching of **CP1** by PA.

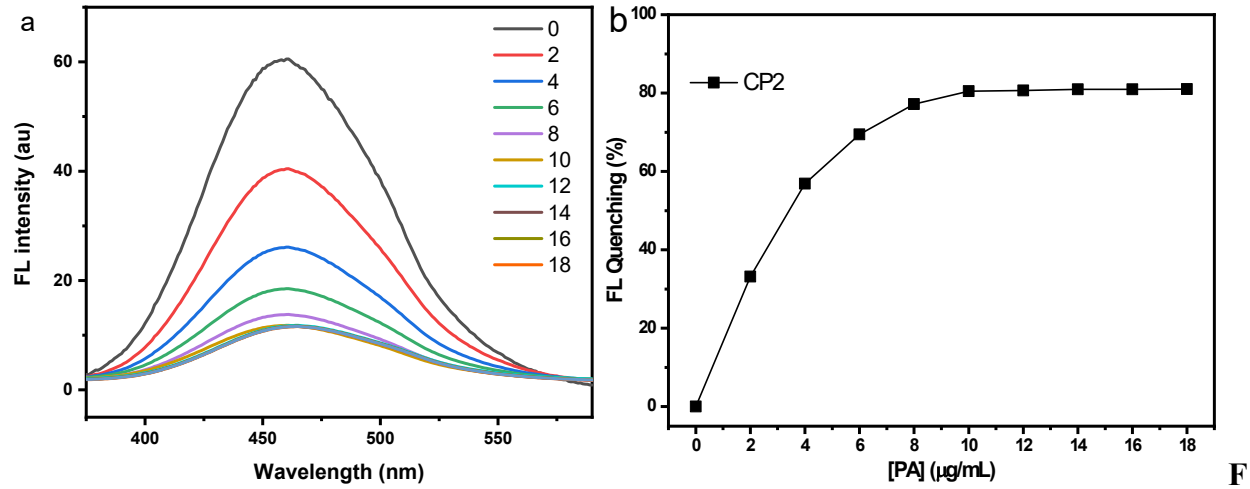

igure S11. Fluorescence spectra of 100.0 μg•mL^{-1} **CP2** in H_2O in the presence of different PA concentrations (μg•mL^{-1}). (B) Concentration-dependent fluorescence quenching of **CP2** by PA.

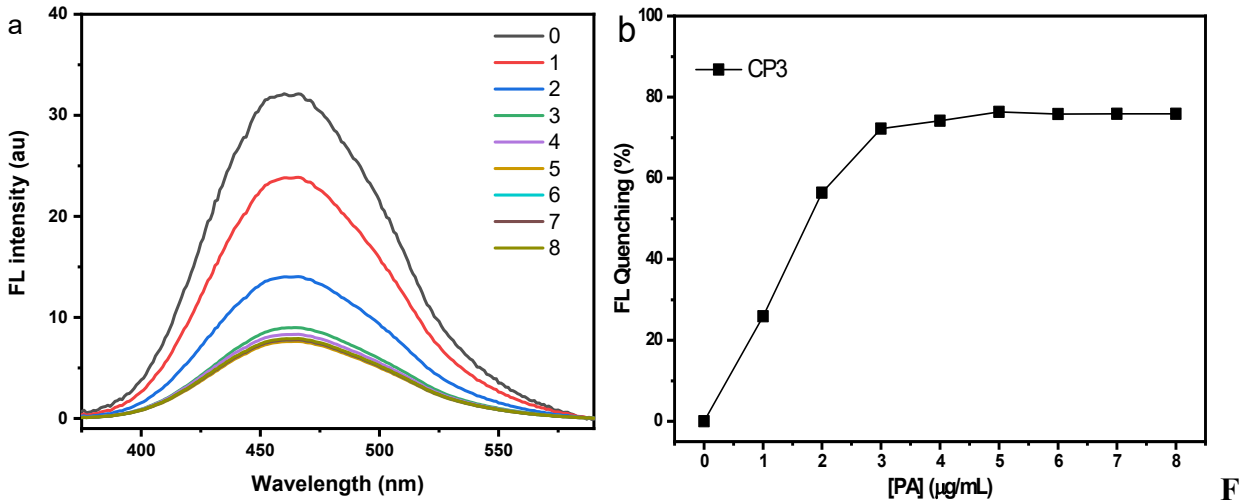

igure S12. Fluorescence spectra of 100.0 μg•mL^{-1} **CP3** in H_2O in the presence of different PA concentrations (μg•mL^{-1}). (B) Concentration-dependent fluorescence quenching of **CP3** by PA.

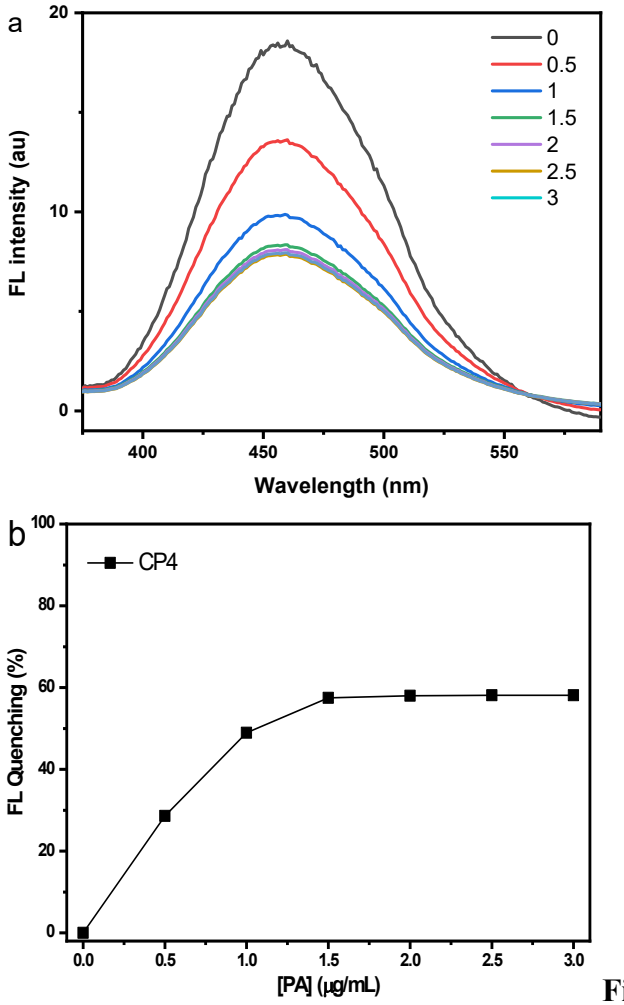

Figure S13. Fluorescence spectra of 100.0 μg•mL-

[1] **CP4** in H_2O in the presence of different PA concentrations (μg•mL^{-1}). (B) Concentration-dependent fluorescence quenching of **CP4** by PA.

Comment [HZ]:

Table S1. Summary of K_{sv} of **CP1** on nitroaromatics detection.

	K_{sv} (Before collapsing-swelling process, M^{-1})	Detection limit (Before collapsing-swelling process, ppm)	K_{sv} (After collapsing-swelling process, M^{-1})	Detection limit (After collapsing-swelling process, ppm)
PA	3.25×10^5	6.0	2.35×10^6	0.25
TNT	2.30×10^4	12.0	1.49×10^5	3.0
DNT	1.77×10^4	14.0	1.15×10^5	4.0
NT	1.36×10^4	14.5	8.86×10^4	4.5

Table S2. Summary of K_{sv} of **LP1** on nitroaromatics detection.

	K_{sv} (Before collapsing-swelling process, M^{-1})	Detection limit (Before collapsing-swelling process, ppm)	K_{sv} (After collapsing-swelling process, M^{-1})	Detection limit (After collapsing-swelling process, ppm)
PA	1.07×10^5	12.0	5.61×10^5	3.0
TNT	1.83×10^4	14.0	1.15×10^5	3.5
DNT	1.23×10^4	15.0	8.14×10^4	4.0
NT	1.08×10^4	16.0	5.57×10^4	4.5

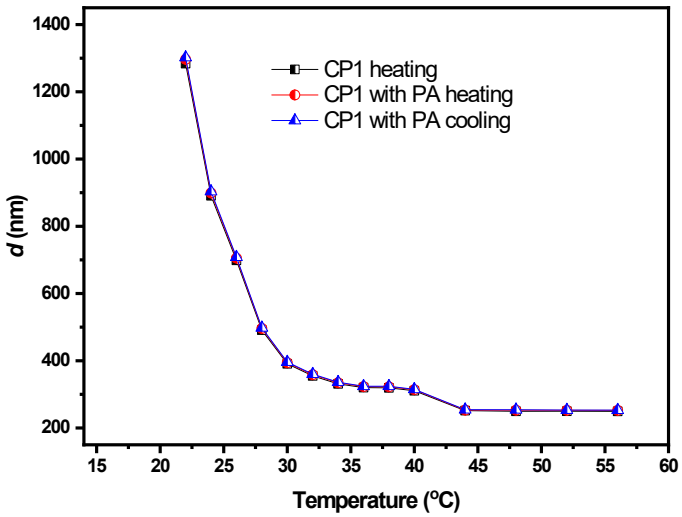

Figure S14. The particle size *vs* temperature of **CP1** with PA during the collapsing-swelling process. [**CP1**] = 0.5 mg/mL, [PA] = 0.1 mg/mL.

Table S3. Summary for the performance of AIE polymers for explosive detection.

Polymer	Structure of polymer	State of analyte	Explosives/nitro-compounds	K_{sv} (M^{-1})	Sensitivity
1	Linear conjugated	Solution	PA, TNT, DNT, NT	1.80×10^5 – 3.65×10^3	5 ppb
		Vapor	TNT, DNT, NT	-	5 ppb
2	Hyper-branched conjugated	Solution	PA	1.67×10^4	0.5 ppm
3	Linear non-conjugated	Solution	PA, TNT, NT	1.57×10^4, 1.29×10^4, 3410	22.9, 22.7, 18.2 ppm
4	Linear non-conjugated	Vapor	TNT, DNT, NT	-	5 ppb, 100 ppb
5	Linear non-conjugated	Solution	PA	1.60×10^5	0.02 ppm
6	Hyper-branched non-conjugated	Solution	PA, TNT	-	0.5 ppm, 1 ppm
		Solid	PA, TNT	-	50 ppm, 100 ppm
CP1*	Linear non-	Solution	PA, TNT, DNT, NT	2.35×10^6	0.25 ppm

	conjugated				

*Current work.

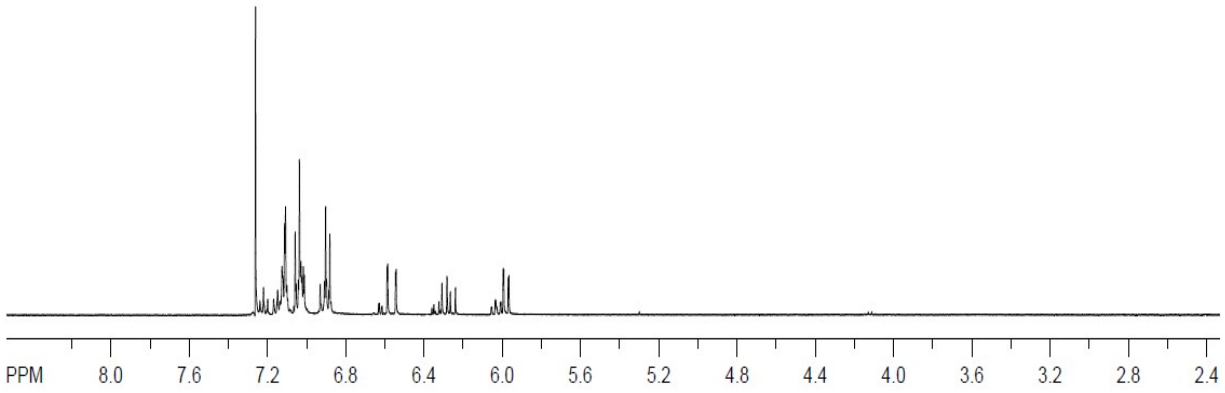

Figure S15. ^{1}H NMR spectrum of monomer (**M2**).

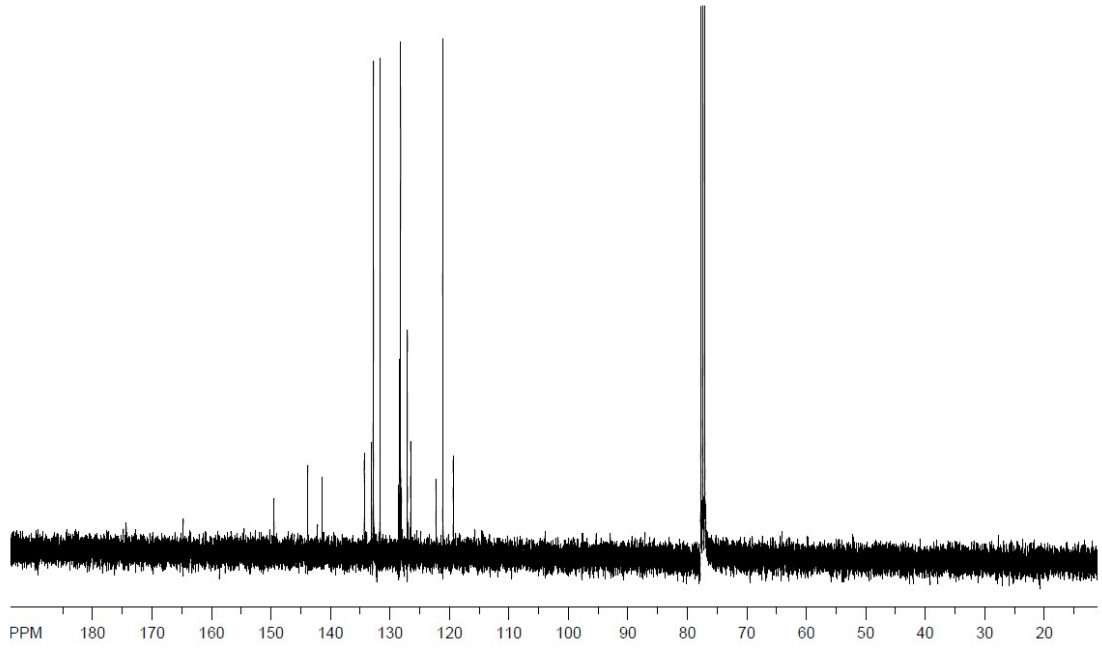

Figure S16. ^{13}C NMR spectrum of monomer (**M2**).

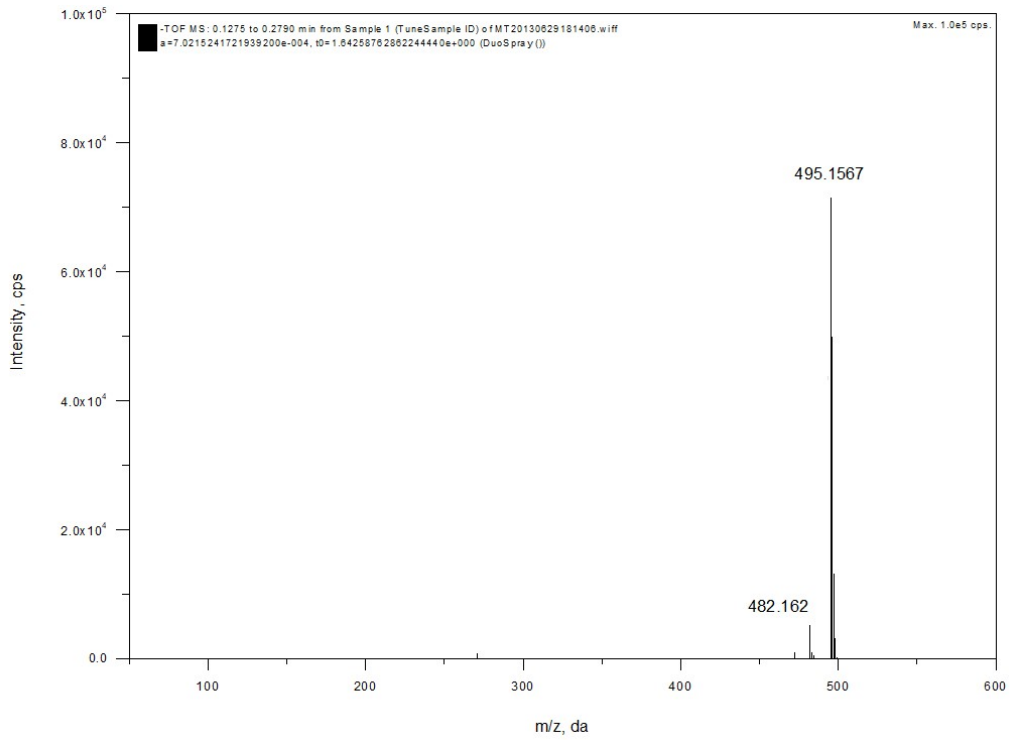

Figure S17. HRMS spectrum of monomer (**M2**).

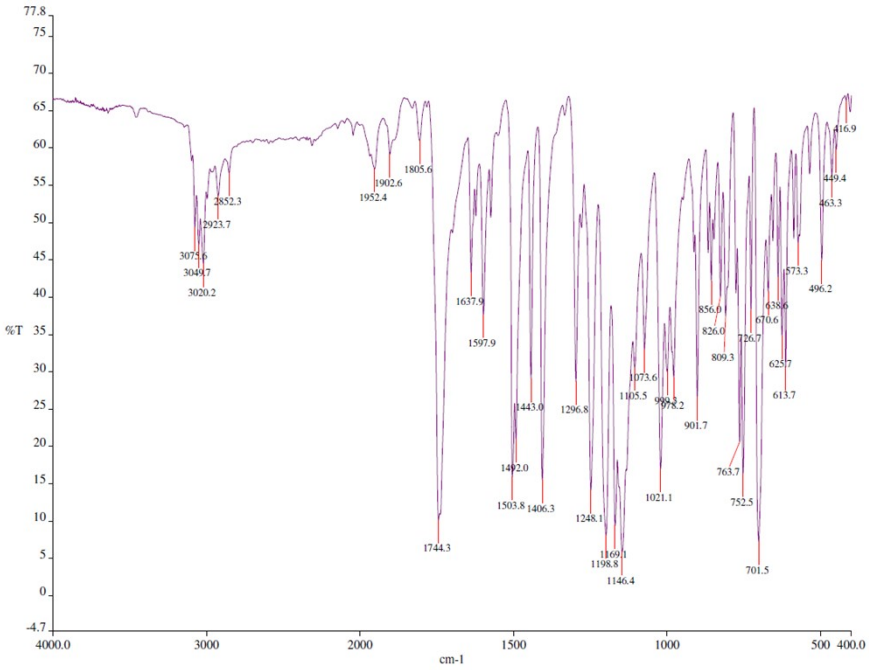

Figure S18. FTIR spectrum of monomer (**M2**).

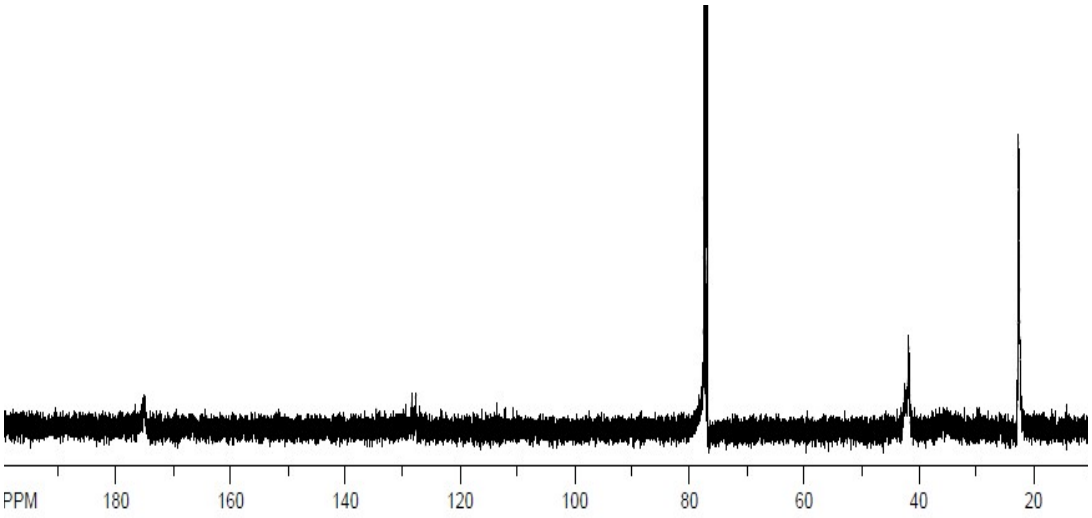

Figure S19. ^{13}C NMR spectrum of **CP1** in $CDCl_3$.

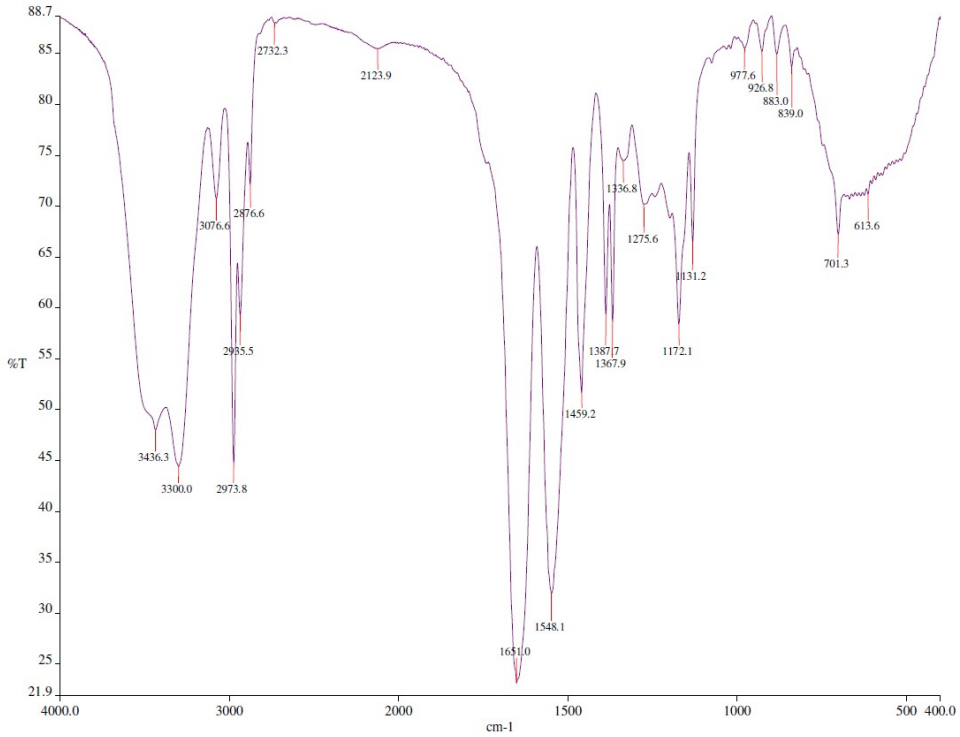

Figure S20. FTIR spectrum of **CP1**.

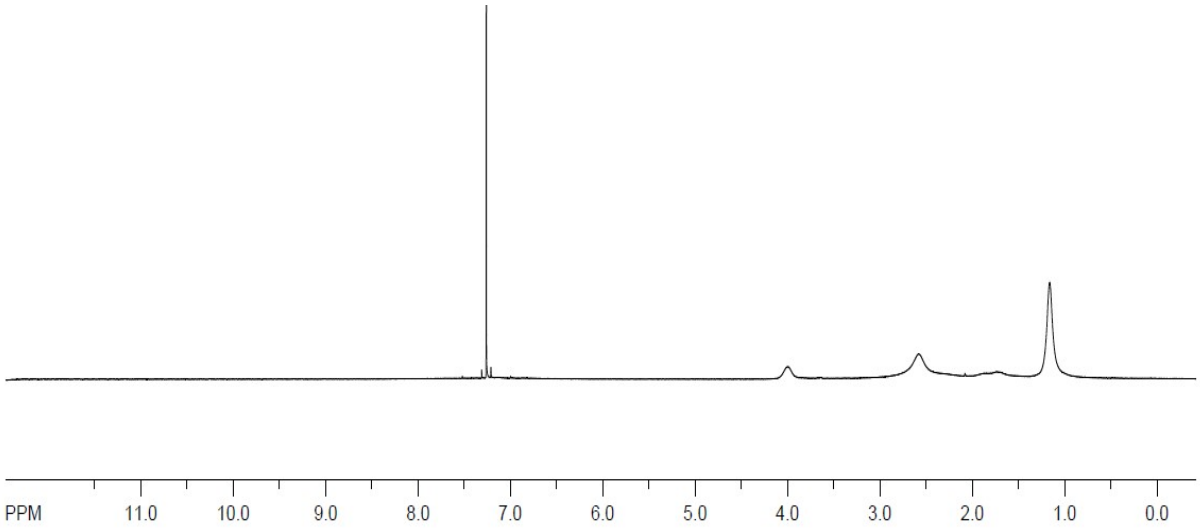

Figure S21. ^{1}H NMR spectrum of **CP2** in $CDCl_3$.

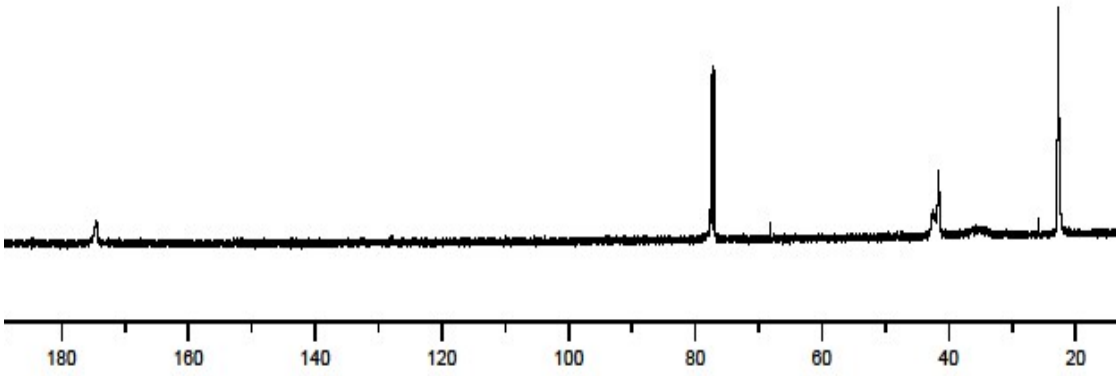

Figure S22. ^{13}C NMR spectrum of **P2** in $CDCl_3$.

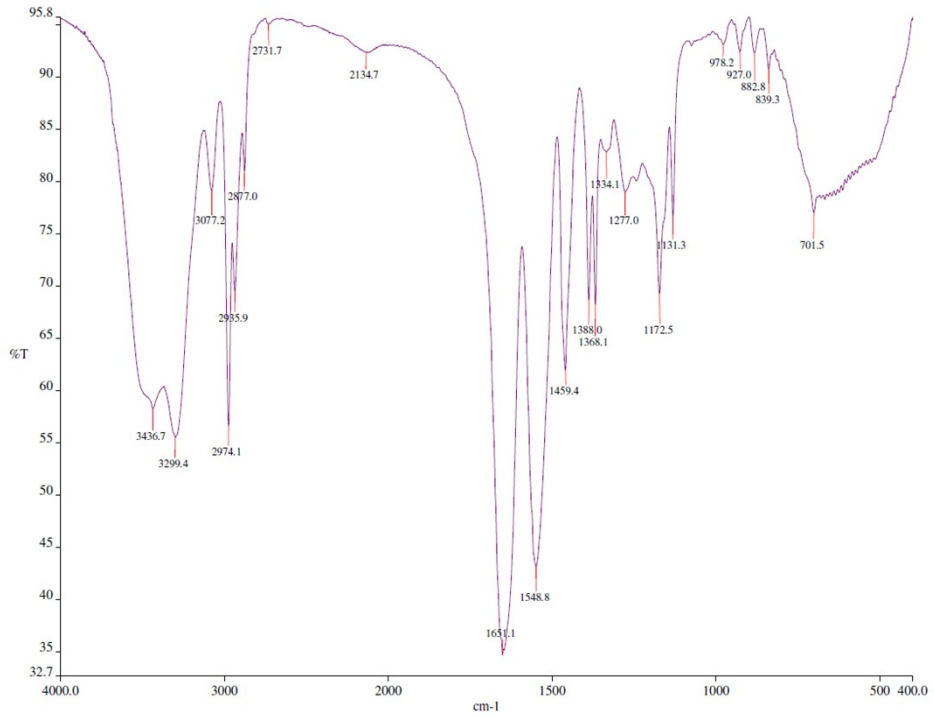

Figure S23. FTIR spectrum of **CP2**.

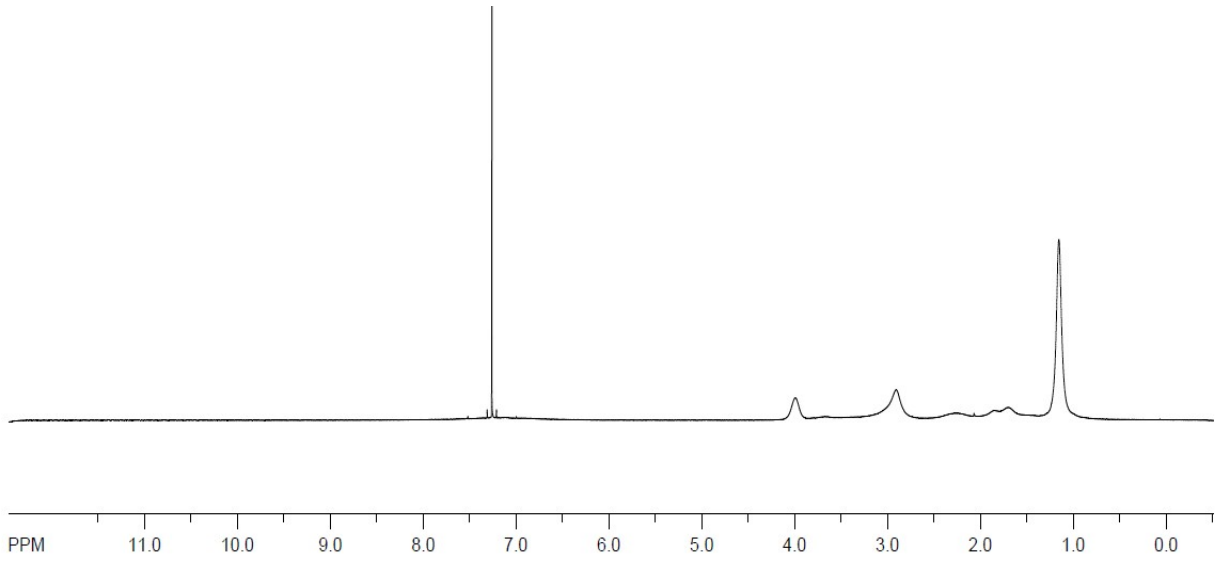

Figure S24. ^{1}H NMR spectrum of **CP3** in $CDCl_3$.

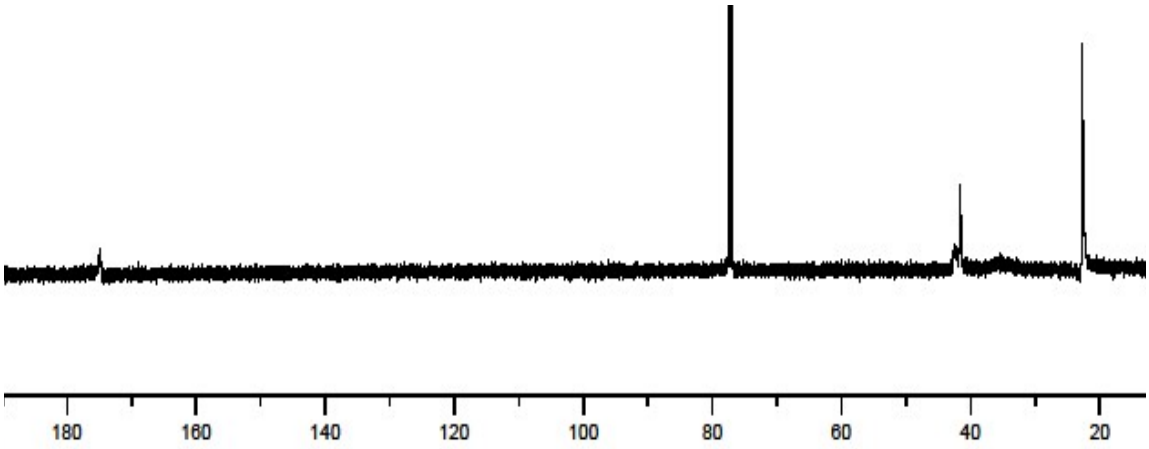

Figure S25. ^{13}C NMR spectrum of **CP3** in $CDCl_3$.

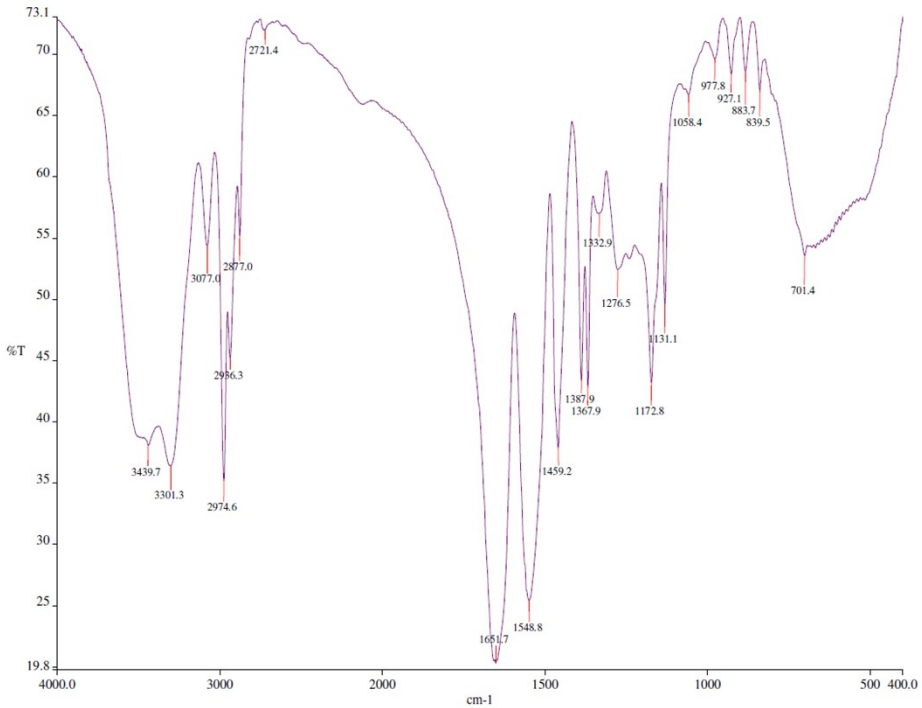

Figure S26. FTIR spectrum of **CP3**.

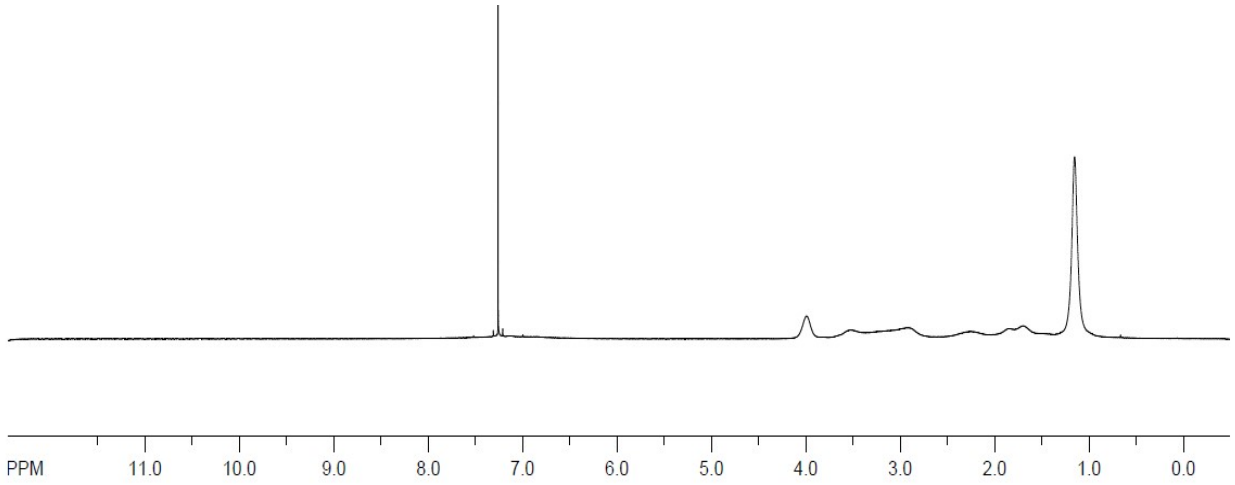

Figure S27. ^{1}H NMR spectrum of **CP4** in $CDCl_3$.

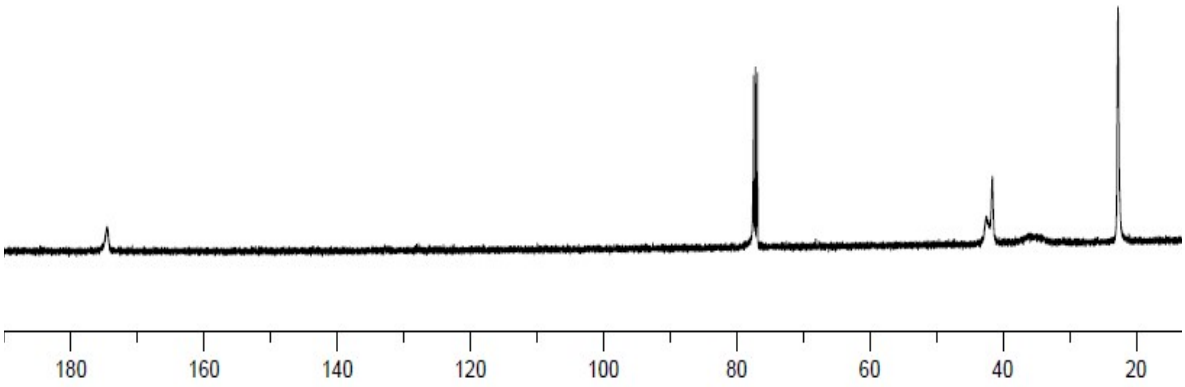

Figure S28. ^{13}C NMR spectrum of **CP4** in $CDCl_3$.

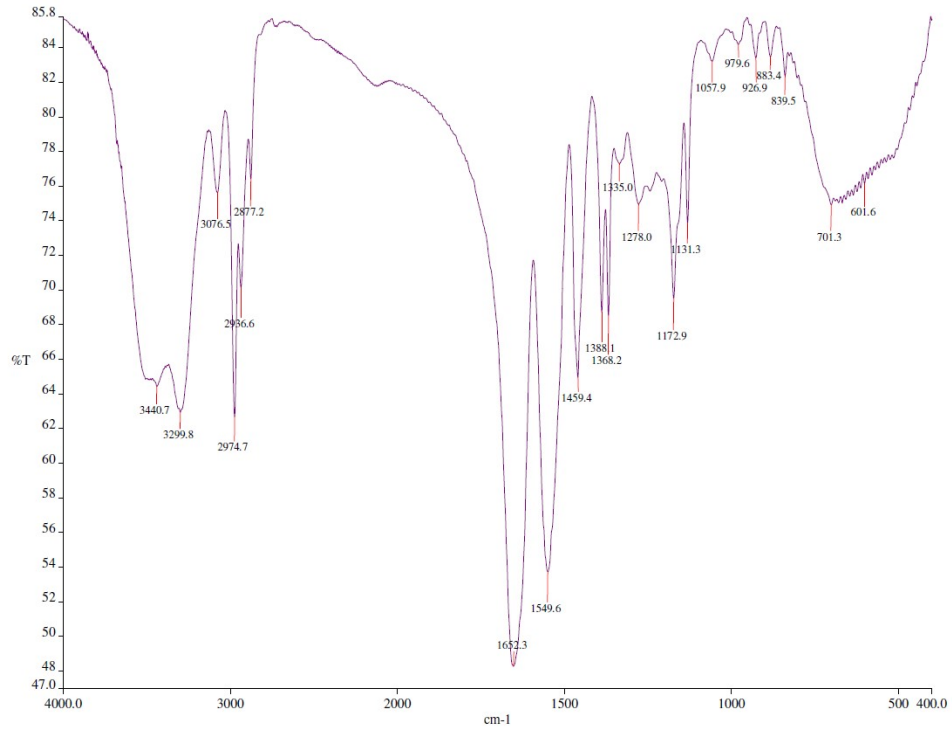

Figure S29. FTIR spectrum of **CP4**.

REFERENCES

(1) M. V. Ramakrishnam Raju, H.-C. Lin, *Org. lett.*, 2014, **16**, 5564.

(2) H. Zhou, X. Wang, T. T. Lin, J. Song, B. Z. Tang and J. Xu, *Polym. Chem.*, 2016, **7**, 6309–6317.

(3) W. Z. Yuan, R. Hu, J. W. Y. Lam, N. Xie, C. K.W. Jim and B. Z. Tang, *Chem. Eur. J.*, 2012, **18**, 2847-2856.

(4) M. H. Chua, H. Zhou, T. T. Lin, J. Wu, J. W. Xu, *J. Polym. Sci., Part A: Polym. Chem.*, 2017, **55**, 672–681.

(5) H. Zhou, Q. Ye, W. T. Neo, J. Song, H. Yan, Y. Zong, B. Z. Tang, T. S. Andy Hor and J. Xu, *Chem. Commun.*, 2014, **50**, 13785—13788.

(6) Q. Wang, M. Chen, B. Yao, J. Wang, J. Mei, J. Z. Sun, A. Qin, B. Z. Tang, *Macromol. Rapid Commun.*, 2013, **34**, 796−802.

(7) X.-M. Hu, Q. Chen, D. Zhou, J. Cao, Y.-J. He and B.-H. Han, *Polym. Chem.*, 2011, **2**, 1124–1128.